Electronic Supplementary Material (ESI) for Soft Matter.
This journal is © The Royal Society of Chemistry 2015

Supplementary Information for

Glassy dynamics of Poly(2-Vinyl-Pyridine) brushes with varying grafting density

Nils Neubauer, René Winkler, Martin Tress, Petra Uhlmann, Manfred Reiche, Wycliffe Kiprop Kipnusu and Friedrich Kremer

Reference measurements of a thin film of PGMA

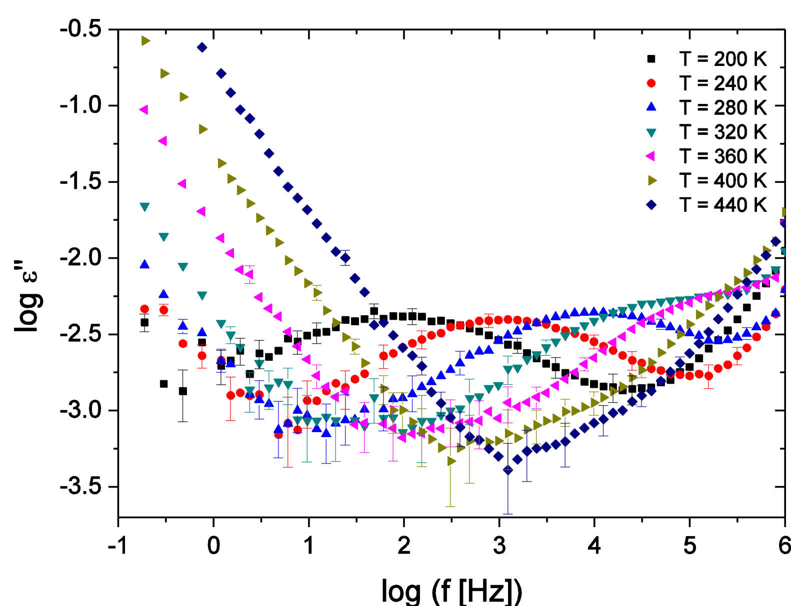

Figure S1: Dielectric loss ε" *versus* frequency for a PGMA layer (thickness: 2.5±1 nm) deposited on a Si-wafer and measured at temperatures as indicated. Besides a relaxation process two conductivity contributions, on the low and high-frequency side are observed being attributed to charge transport in the sample material or the spacers and in the wafer material itself. The relative experimental accuracy is given by the size of the symbols if not indicated otherwise.

In order to identify the different processes in the dielectric loss ε" spectra of the bilayer system consisting of a PGMA anchoring layer and the P2VP polymer brush, reference measurements of a single layer of PGMA are carried out. The samples are prepared on 10x20 mm^2 Si-wafer dice (purchased from Si-Mat with a specific resistance ρ<0.01 Ωcm and a 200-nm-thick Al-layer on the backside). For cleaning the wafer dice is ultrasonicated in an ethanol bath and treated with oxygen plasma. Afterwards, from a 0.02wt% chloroform solution, a PGMA layer (M_n = 17.5 kg/mol, M_W = 29.7 kg/mol, obtained from Polymer Source Inc.) is deposited by spin-coating and annealed at 100°C for 20 min. The film thickness is d_{PGMA} = 2.5±0.1 nm, as measured by ellipsometry (Sentech SE-402 scanning microfocus ellisometer). For dielectric measurements a Novocontrol System Concept 20 (frequency range: 10^{-1} Hz - 10^{6} Hz, temperature range: 200 K - 440 K) in combination with nanostructured electrodes is employed. Figure S1 shows spectra at selected temperatures of the PGMA layer. At the low frequency side, a linear contribution in log-log representation can be observed, originating from charge transport due to impurities in the sample or imperfect silica spacers of the nanostructured top-electrode. At the high frequency side there is another conductivity contribution due to the limited resistivity of

the Si-wafer material itself (see next section of the SI). Between these two linear conductivity contributions, a PGMA relaxation process is observed.

The contribution of the electrodes at high frequencies and a polarization process at low frequencies

In the following the assignment of the different contributions in the dielectric loss ε" spectra shown in Figure 3 is described in detail. As described above, a PGMA-relaxation is measured and located between 10^5 Hz and 10^6 Hz. Furthermore, the two linear contributions at the low and high frequency side are present which originate from a parasitic conductivity (probably related to the silica spacers or contaminating particles between the electrodes) and the limited conductivity of the silicon electrodes, respectively. Beyond this, two further processes are observed. That one at higher frequencies is assigned to the α-relaxation of P2VP while the other one represents a polarization emerging from the conductivity in P2VP.

The latter effect can be explained in terms of an equivalent circuit[1] (Figure S2 c), accounting for the particular build-up of the sample. For clarity, the PGMA layer is neglected at first and hence the circuit is described by

$$\frac{D}{\varepsilon^*_{total}} = 2\frac{d_W}{\varepsilon^*_W} + \frac{d_{sp}}{\rho_{sp}\varepsilon^*_{sp} + 1 - \rho_{sp}} + \frac{d_{gap}}{\varepsilon^*_{gap}} + \frac{d_p}{\varepsilon^*_p} + \frac{d_o}{\varepsilon^*_o} \tag{1}$$

where D and $\varepsilon^*_{total} = \varepsilon'_{total} + i\varepsilon''_{total}$ are the thickness and the complex dielectric function of the sample in total while d_c and ε^*_c are the same quantities of each component with c representing the indices W, sp, gap, p and o for the silicon electrode (wafer), the spacers, the gap, the polymer and the interfacial oxide, respectively. ρ_{sp} is the proportion of the area covered by spacers.

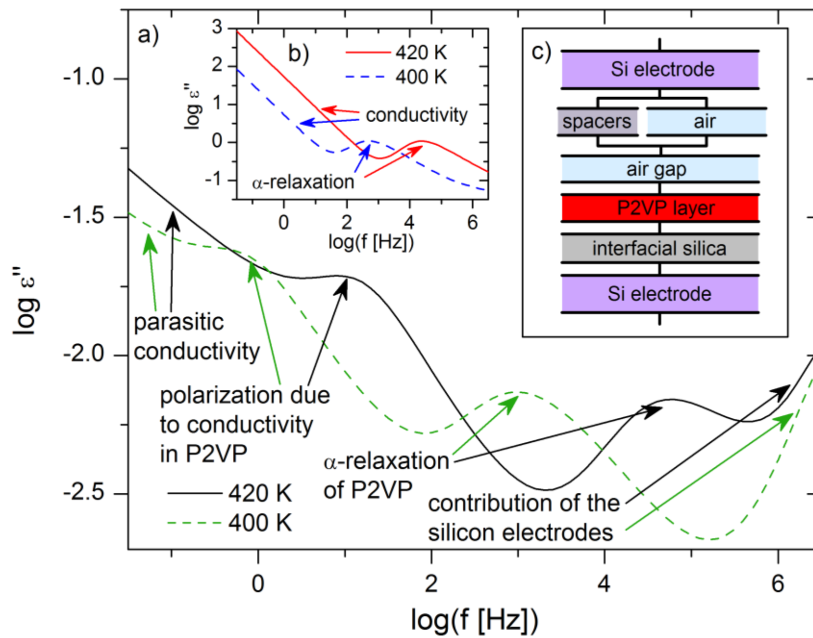

Figure S2: a) Dielectric loss ε" spectra of an equivalent circuit modeling a 6.4-nm-thick P2VP layer (with bulk properties) in a nanostructured electrode arrangement at two different temperatures as indicated. The geometrical parameters for this calculation are: 35 nm spacer height, 5 µm spacer width, 45 µm spacer separation (lateral distance between spacers yielding a proportion of 1% covered by spacers), 10 nm air gap height, 6.4 nm P2VP layer thickness, 1.4 nm interfacial silica thickness summing up to a total distance of 52.8 nm resembling a capacity of 183 pF on an area of 1 mm^2. The silicon electrodes, with a thickness of 600 µm each, do not contribute to the spectra in the frequency range below ~100 kHz due to their high conductivity in this range ($\varepsilon'' = \sigma_{Si}/(\varepsilon_0\ 2\pi\ f)$ where ε_0 represents the permittivity of vacuum and σ_{Si} the

conductivity of the doped silicon $\sigma_{Si} = 4\cdot10^{2}$ S/cm). In contrast, above 100 kHz a characteristic contribution is caused by the particular shape of the permittivity (based on measurements of the electrode material as described by ε' = f/3.2 for f ≥ 10 kHz and ε' = 3. $2\cdot10^{7}$/f for f ≤ 10 kHz). For the dielectric properties the following values are taken: ε' = 1, ε" = 0 for air; ε' = 4, ε" = σ(T)/(ε_0 2π $f^{0.3}$) ·$(1\ \mathrm{Hz})^{-0.7}$ for the silica parts (interfacial silica and spacers), where σ(T) is the temperature dependent conductivity (σ(420 K) = $3.2\cdot10^{-11}$ S/cm and σ(400 K) = $2\cdot10^{-11}$ S/cm); bulk properties for the P2VP layer. b) Dielectric loss ε" spectra of bulk P2VP are assumed to calculate the curves shown in a). c) Scheme of the equivalent circuit underlying the calculations.

Figure S2 a) displays the result of the calculations according to equ. (1) for two different temperatures, which contain all contributions known from the measured spectra (Figure 3), except for the relaxation of the PGMA. The geometrical measures of the sample are determined by AFM and ellipsometry (silicon electrode thickness ~600 µm, thickness of the native silica layer at the bottom electrode 1.4 nm, height and horizontal separation of the silica spacers 35 nm and 45 µm, respectively). Additionally, a gap between bottom electrode and spacers of 10 nm has been inserted to achieve the capacitance of the sample of ~180 pF. This gap is presumably the result of the surface roughness of the electrodes. This demonstrates that a component exhibiting just one molecular relaxation and a conductivity contribution (Figure S2 b) in the examined frequency and temperature range causes, in that particular sample arrangement, two processes in the total dielectric loss spectrum. The conductivity of the P2VP layer gives rise to the additional process below the α-relaxation (Figure S2 a).

Model function to fit the spectra

Since equ. (1) describes all features observed in the measured spectra, it is used as a fit function to extract the net dielectric properties of the components, e.g. the P2VP brushes. To account for the PGMA layer a further term is added so that the equation reads

$$\frac{D}{\varepsilon^*_{total}} = 2\frac{d_W}{\varepsilon^*_W} + \frac{d_{sp}}{\rho_{sp}\varepsilon^*_{sp} + 1 - \rho_{sp}} + \frac{d_{gap}}{\varepsilon^*_{gap}} + \frac{d_{P2VP}}{\varepsilon^*_{P2VP}} + \frac{d_{PGMA}}{\varepsilon^*_{PGMA}} + \frac{d_o}{\varepsilon^*_o} \tag{2}$$

with the same notion like in equ. (1) except for the indices P2VP and PGMA indicating the thickness and complex dielectric permittivity of the respective polymer layer. The polymer components are each described by a Havriliak-Negami function with a conductivity term

$$\varepsilon^*_p = \varepsilon'_p - i\varepsilon''_p = \varepsilon_\infty + \frac{\Delta\varepsilon}{\left(1+\left(\omega\tau_{HN}\right)^{\alpha}\right)^{\beta}} - i\frac{a\sigma_{DC}}{\varepsilon_0\omega^s} \tag{3}$$

with the dielectric strength Δε, the parameter for symmetric and asymmetric broadening α and β, respectively, the relaxation time τ_{HN}, the angular frequency ω=2πf, DC conductivity σ_{DC}, the permittivity of the vacuum ε_0, the slope parameter s and the parameter $a=1\mathrm{Hz}^{s-1}$ to correct for the units. In case of the PGMA, the final term of equ. (3) is not implemented since there is no indication for a conductivity contribution in this material. For the silica components, a constant permittivity is assumed, while the dielectric loss contains a parasitic conductivity

$$\varepsilon^*_{sp} = \varepsilon^*_o = \varepsilon'_o - i\frac{a\sigma_{DC}}{\varepsilon_0\omega^s} \tag{4}$$

The dielectric function of the silicon wafers is approximated by the equation

$$\varepsilon_W^* = \varepsilon_W' - i\varepsilon_W'' = 10^{|\log f - 4| + 3.5} - i\,10^{12.86 - \log f} \tag{5}$$

according to measurements of a single silicon electrode.

Tables S1 & S2 summarize the parameters of the fits curves shown in Figure 3.

Table S1: Geometrical constants in the fit functions shown in Figure 3.

sample	D [nm]	d_{PGMA} [nm]	d_{P2VP} [nm]	d_o [nm]	d_{gap} [nm]	d_W [µm]	d_{sp} [nm]	ρ_{sp}
1	52	2.5	7.1	1.4	2	600	35	0.01
2	45	2.5	6.4	1.4	5	600	35	0.01
3	58	2.5	5.2	1.4	13	600	35	0.01
4	77	2.5	4.5	1.4	27	600	35	0.01
5	53	2.5	1.8	1.4	14.5	600	35	0.01

Table S2: Fit parameters of the PGMA, P2VP and silica components in the fit functions shown in Figure 3 (the values of ε_∞ for PGMA and P2VP as well as ε' of the silica have been fixed).

		PGMA					P2VP							silica		
sample	T [K]	ε_∞	$\Delta\varepsilon$	α	β	τ_{HN} [s]	ε_∞	$\Delta\varepsilon$	α	β	τ_{HN} [s]	σ_{DC} [S/cm]	s	ε'	σ_{DC} [S/cm]	s
1	420	1.75	20.0	0.38	0.36	$1.1 \cdot 10^{-6}$	2.9	2.6	0.96	0.37	$4.8 \cdot 10^{-5}$	$9.8 \cdot 10^{-10}$	0.58	4	$7.9 \cdot 10^{-11}$	0.26
	410	1.75	14.6	1.00	0.62	$4.9 \cdot 10^{-6}$	2.9	3.5	1.00	0.35	$3.1 \cdot 10^{-4}$	$4.1 \cdot 10^{-10}$	0.54	4	$6.4 \cdot 10^{-11}$	0.27
	400	1.75	20.0	0.43	0.41	$2.5 \cdot 10^{-6}$	2.9	2.8	1.00	0.29	$3.8 \cdot 10^{-3}$	$1.2 \cdot 10^{-10}$	0.42	4	$5.0 \cdot 10^{-11}$	0.35
2	420	1.75	10.0	0.65	0.65	$6.9 \cdot 10^{-7}$	2.9	5.7	0.79	0.28	$9.6 \cdot 10^{-5}$	$1.3 \cdot 10^{-9}$	0.71	4	$5.0 \cdot 10^{-11}$	0.35
	410	1.75	2.5	1.00	0.46	$1.2 \cdot 10^{-6}$	2.9	6.1	1.00	0.31	$4.5 \cdot 10^{-4}$	$5.6 \cdot 10^{-10}$	0.80	4	$3.4 \cdot 10^{-11}$	0.33
	400	1.75	10.0	0.60	0.60	$1.8 \cdot 10^{-6}$	2.9	5.0	0.94	0.36	$2.1 \cdot 10^{-3}$	$1.5 \cdot 10^{-10}$	0.80	4	$2.8 \cdot 10^{-11}$	0.35
3	420	1.75	4.5	0.86	0.64	$1.1 \cdot 10^{-6}$	2.9	3.1	0.75	0.34	$1.4 \cdot 10^{-5}$	$5.3 \cdot 10^{-10}$	0.42	4	$1.3 \cdot 10^{-10}$	0.56
	410	1.75	13.6	0.69	0.52	$1.1 \cdot 10^{-6}$	2.9	2.7	0.90	0.28	$1.2 \cdot 10^{-4}$	$2.8 \cdot 10^{-10}$	0.43	4	$9.6 \cdot 10^{-11}$	0.67
	400	1.75	20.0	0.74	0.55	$1.1 \cdot 10^{-6}$	2.9	2.3	1.00	0.32	$5.9 \cdot 10^{-4}$	$2.4 \cdot 10^{-10}$	0.49	4	$7.7 \cdot 10^{-11}$	0.86
4	420	1.75	20.0	0.63	0.63	$1.1 \cdot 10^{-6}$	2.9	2.6	0.50	0.24	$2.0 \cdot 10^{-5}$	$2.4 \cdot 10^{-10}$	0.38	4	$1.3 \cdot 10^{-10}$	0.53
	410	1.75	14.9	1.00	0.78	$1.1 \cdot 10^{-6}$	2.9	2.4	0.83	0.19	$1.7 \cdot 10^{-4}$	$8.3 \cdot 10^{-11}$	0.25	4	$7.3 \cdot 10^{-11}$	0.56
	400	1.75	20.0	1.00	0.77	$1.1 \cdot 10^{-6}$	2.9	0.4	0.46	0.29	$4.5 \cdot 10^{-5}$	$1.1 \cdot 10^{-11}$	0.12	4	$5.1 \cdot 10^{-11}$	0.60
5	420	1.75	86.2	0.41	2.44	$1.3 \cdot 10^{-6}$	2.9	2.7	1.00	0.07	$1.4 \cdot 10^{-4}$	$2.0 \cdot 10^{-10}$	0.31	4	$6.8 \cdot 10^{-12}$	0.40
	410	1.75	6.7	1.54	1.84	$2.2 \cdot 10^{-7}$	2.9	1.0	1.00	0.07	$5.4 \cdot 10^{-4}$	$7.1 \cdot 10^{-11}$	0.29	4	$2.7 \cdot 10^{-12}$	0.98
	400	1.75	11.1	1.00	0.47	$4.3 \cdot 10^{-6}$	2.9	8.7	0.21	0.98	$1.6 \cdot 10^{-3}$	$2.8 \cdot 10^{-9}$	0.98	4	$5.9 \cdot 10^{-12}$	0.21

References

1. M. Tress et al. in F. Kremer, (Ed.), *Dynamics in Geometrical Confinement*, Advances in Dielectrics, Springer, 2014